# Experimental and simulation studies on focused ultrasound triggered drug delivery

**Zhen Jin**[1]
**Yongjin Choi**[2]
**Seong Young Ko**[1,2]
**Jong-Oh Park**[1,2]
**Sukho Park**[1,2*]

[1] *Department of Mechanical Engineering, Chonnam National University, Gwangju, Korea*

[2] *Robot Research Initiative, Chonnam National University, Gwangju, Korea*

## Abstract

To improve drug delivery efficiency in cancer therapy, many researchers have recently concentrated on drug delivery systems that use anticancer drug loaded micro- or nanoparticles. In addition, induction methods, such as ultrasound, magnetic field, and infrared light, have been considered as active induction methods for drug delivery. Among these, focused ultrasound has been regarded as a promising candidate for the active induction method of drug delivery system because it can penetrate a deep site in soft tissue, and its energy can be focused on the targeted lesion. In this research, we employed focused ultrasound as an active induction method. For an anticancer drug loaded microparticles, we fabricated poly-lactic-co-glycolic acid docetaxel (PLGA-DTX) nanoparticle encapsulated alginate microbeads using the single-emulsion technique and the aeration method. To select the appropriate operating parameter for the focused ultrasound, we measured the pressure and temperature induced by the focused ultrasound at the focal area using a needle-type hydrophone and a digital thermal detector, respectively. Additionally, we conducted a simulation of focused ultrasound using COMSOL Multiphysics 4.3a. The experimental measurement results were compared with the simulation results. In addition, the drug release rates of the PLGA-DTX-encapsulated alginate microbeads induced by the focused ultrasound were tested. Through these experiments, we determined that the appropriate focused ultrasound parameter was peak pressure of 1 MPa, 10 cycle/burst, and burst period of 20 $\mu$Sec. Finally, we performed the cell cytotoxicity and drug uptake test with focused ultrasound induction and found that the antitumor effect and drug uptake efficiency were significantly enhanced by the focused ultrasound induction. Thus, we confirmed that focused ultrasound can be an effective induction method for an anticancer drug delivery system.  Volume 64, Number 1, Pages 134–142, 2017

***Keywords:*** *focused ultrasound, cavitation effect, sonoporation, PLGA-DTX encapsulated alginate microbeads*

## 1. Introduction

Today, cancer treatment still relies on radiotherapy, chemotherapy, medication, and surgical removal of tumors. Among these treatments, chemotherapy using anticancer drugs is considered the conventional method but can cause systemic toxicities and other side effects in normal tissues and organs [1, 2]. To overcome these toxicities and side-effects and to increase drug delivery efficiency, many researchers have studied anticancer drugs loaded nano- and microcarriers and specific exogenous stimuli-induced drug delivery systems [3–5]. The drug-loaded carrier should contain a sufficient quantity of anticancer drugs, have an adequately long shelf-life, and be nontoxic in substance. After targeting the tumor with drug-loaded carriers, the drug release rate can be also controlled by specific stimuli, such as infrared light, temperature, pH, alternating magnetic field, and ultrasound [6–9]. These stimuli can induce drug release in the targeted position in an induction method that should have no side effects in the body.

Focused ultrasound has many advantages as a controlled-release drug delivery system and has been widely applied in medicine because it can penetrate deep into soft tissues and can be concentrated at targeted lesions. Focused ultrasound

***Abbreviations:*** *4T1, breast cancer; BCA, bicinchoninic acid; CT26, colon cancer; DCM, dichloromethane; DTX, docetaxel; HPLC, high-performance liquid chromatography; MTT, 3-(4, 5-dimethylthiazol-2-yl)-2, 5-diphenyltetrazolium bromide; PBS, phosphate-buffered saline; PLGA, poly-lactic-co-glycolic acid; PVA, polyvinyl alcohol; PVDF, polyvinylidene fluoride; PZT, piezoelectric lead zirconate titanate; SDS, sodium dodecyl sulfate.*

**Address for correspondence: Sukho Park, Ph.D, Department of Mechanical Engineering, Chonnam National University, Gwangju 500-757, Korea. Tel.: +82 62 530 1687; fax: +82 62 530 0267; e-mail: jop@jnu.ac.kr, spark@jnu.ac.kr.*

*Received 19 May 2015; accepted 25 October 2015*

*DOI: 10.1002/bab.1453*

*Published online 14 April 2016 in Wiley Online Library (wileyonlinelibrary.com)*

can trigger drug release through heat, acoustic streaming, and the cavitation effect [10, 11]. In addition, focused ultrasound can improve the drug uptake of the targeted tumor tissue by increasing cell membrane permeability with sonoporation [12]. However, sonication with a low-frequency ultrasound can easily cause tissue damage through inertial cavitation [13]. When ultrasound raises the tissue temperature above 43 °C, vascular shutdown can occur. To enhance drug delivery efficiency without tissue damage, it has been reported that the extravasation of therapeutic agents due to transient cavitation can be enhanced at the ultrasound frequency of 1 MHz and the negative pressure of 0.5 Mpa without producing tissue damage [14, 15]. Therefore, the appropriate ultrasound parameters should be used to enhance drug delivery.

In this research, as drug-loaded carriers, we fabricated poly-lactic-co-glycolic acid docetaxel (PLGA-DTX) nanoparticles encapsulated with alginate microbeads. To select the appropriate parameters of the focused ultrasound for drug delivery, the pressure and temperature in a target region induced by focused ultrasound were measured. The experimental results were compared with the simulation results using COMSOL Multiphysics 4.3a. We evaluated the triggered drug release performance using focused ultrasound and selected the appropriate parameter of focused ultrasound based on the previous experimental results. Then, the cytotoxicity and drug uptake efficiency was tested using focused ultrasound with selected parameter. Finally, we confirmed that PLGA-DTX-encapsulated alginate microbeads combined with focused ultrasound sonication can produced an enhanced antitumor effect.

## 2. Materials and Methods

### 2.1. Synthesis of PLGA-DTX-encapsulated alginate microbeads

We synthesized PLGA-DTX encapsulated alginate microbeads through the single-emulsion technique [16] and the aeration method [17]. First, to fabricate the PLGA-DTX nanoparticles, 10 mg of DTX was dissolved in 2 mL of dichloromethane (DCM), and 100 mg of PLGA wsa added to the solution. Then, the oil solution was added to 40 mL of polyvinyl alcohol (PVA) solution (1% w/v), and the mixture solution was emulsified for 10 Min with a probe sonicator at 300 W. After emulsification, the oil-in-water emulsion was magnetically stirred for 8 H to evaporate the DCM. After centrifugation of the solution, the supernatant was discarded, and the precipitate was washed with deionized water. The centrifugation and washing processes were repeated three times. Finally, after washing with distilled water and freeze-drying for 48 H, the powder form of PLGA-DTX nanoparticles was obtained.

Next, the PLGA-DTX powder was distributed in a 2% alginate solution and poured into an aeration device chamber. The mixture solution was nebulized at an air flow rate of 250 sccm, which formed alginate droplets. The alginate droplets were cross-linked by the calcium ion from the calcium chloride bath, and alginate microbeads formed. Then, the alginate microbead distributed solution was centrifuged, and the precipitate was washed by deionized water. After the centrifugation and washing processes were repeated three times, the precipitate was mixed with 5 mL of deionized water and lyophilized for 48 H. Finally, 1 mg of drug-loaded alginate microbeads was prepared to test the drug encapsulation efficiency with the high-performance liquid chromatography (HPLC) method.

### 2.2. Focused ultrasound and measurement of induced pressure and temperature

As shown in Fig. 1, a single-element focused ultrasound transducer (aperture diameter: 30 mm, focal length: 29.7 mm, frequency: 925 kHz) was used to generate ultrasound, and a function generator (33210A; Agilent, Palo Alto, CA, USA) was employed to create sonication signal. A radio frequency power amplifier (HSA-4014; NF Corporation, Yokohama, Japan) was used to amplify the sonication signal, and a self-assembled external impedance matching circuit was used to match the electric impedance of the transducer with the output impedance of the amplifier.

A needle-type hydrophone and a digital thermocouple were used to measure the pressure and temperature at the focal area of focused ultrasound, respectively. First, the experiment for measuring acoustic pressure was set up as illustrated in Fig. 1a. The focused ultrasound transducer was mounted at the bottom of a Lucite tank (40 × 30 × 25 cm) filled with degassed and deionized water ($T$: 37°C), and focused ultrasound was operated in burst mode with 10 cycle/burst, and a burst period of 20 μSec. The polyvinylidene fluoride (PVDF) needle-type hydrophone with a sensing element of 0.2 mm (Precision Acoustics, Dorchester, UK) was connected to a three-dimensional (3D) XYZ stage in order to position the tip of the PVDF probe at the focal point and a commercial acoustic absorbent rubber was located in the water/air interface to avoid the disturbance from the reflection of ultrasound. The output of the PVDF probe was recorded using a digital oscilloscope (LeCroy Waverunner 204MXI-A; Chestnut Ridge, NY, USA) with a 100 MHz sampling rate, and the recorded data were used for offline pressure calibration and analysis.

Second, the experiment for measuring tissue temperature at the focal point of the focused ultrasound was set up as shown in Fig. 1b. The focused ultrasound system and the input signal were set to the same as previous pressure measurement. A thermometer probe (UT325 thermometer; Uni-Trend Technology, Dongguan, People's Republic of China) was connected with the 3D XYZ stage, and the tip of the thermocouple probe was inserted in the center of degassed swine muscle tissue (30 × 30 × 20 mm) and positioned at the focal point. The focused ultrasound sonication was stopped when the tissue temperature reached 42 °C, or thermal equilibrium occurred before the temperature reached 42 °C.

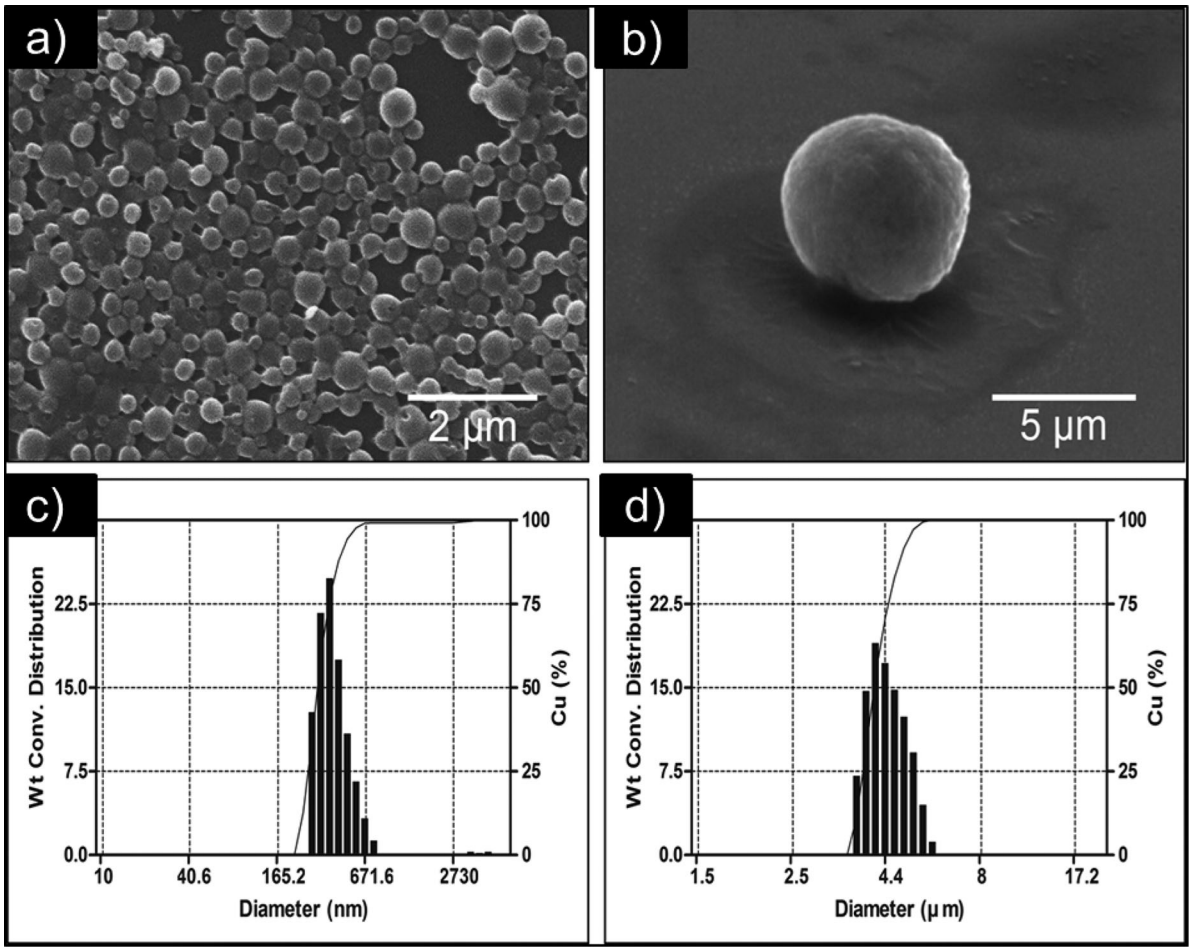


**FIG. 1**

*(a) SEM image of PLGA-DTX nanoparticles, scale bar: 2 μm. (b) SEM image of PLGA-DTX encapsulated alginate microbeads, scale bar: 5 μm. (c and d) Size distribution of PLGA nanoparticles and alginate microbeads.*

### 2.3. COMSOL simulation

To compare the experimental results of focused ultrasound induced pressure and tissue temperature, we executed a COMSOL simulation, in which a two-dimensional model of the focused ultrasound induced pressure was developed. As shown in Fig. 2a, the focused ultrasound transducer was modeled with the two elements of piezoelectric lead zirconate titanate (PZT) ceramics (30 × 2.163 mm) and acoustic lens (30 × 16.837 mm, curvature: 40 mm): the PZT was in the bottom layer, and the acoustic lens was attached to the PZT. In addition, the water chamber domain (40 × 50 mm) was modeled and attached to the transducer, and the boundary of the water domain was set as a perfect boundary layer in order to exclude disturbances from the ultrasound reflection. For the numerical simulation, the model was meshed with 15,691 elements. First, by applying the amplified voltage to the transducer, generated pressure data were obtained in the COMSOL simulation model. Second, to execute the tissue temperature simulation, we included a tissue domain (30 × 20 mm) in the previous model, as shown in Fig. 2c. The input signal for COMSOL simulation was coded with MATLAB, and the sonication time was also set to the same value as in the experiment. All the parameters of the COMSOL simulation are summarized in Table 1 [18–20].

### 2.4. Focused ultrasound triggered drug release

We measured the drug release rate upon focused ultrasound induction by following the protocol in the reference paper [21]. Three sets of samples were prepared by repeating the following process: drug-loaded alginate microbeads with 1 mL phosphate-buffered saline (PBS) buffer solution were poured into each microcentrifuge tube. Then, the samples were immersed in a water tank, fixed with the XYZ axis stage sample holder, and positioned precisely at the focal point of the focused ultrasound transducer. The tank was filled with degassed water, and the temperature was maintained at 37 °C. Next, the sample was sonicated by focused ultrasound for 4 Min. Finally, using the HPLC method, the focused ultrasound drug release rate was measured at different peak pressure and burst period.

### 2.5. Cell culture and cytotoxicity tests

The antitumor effect of PLGA-DTX-encapsulated alginate microbeads combined with focused ultrasound induction was

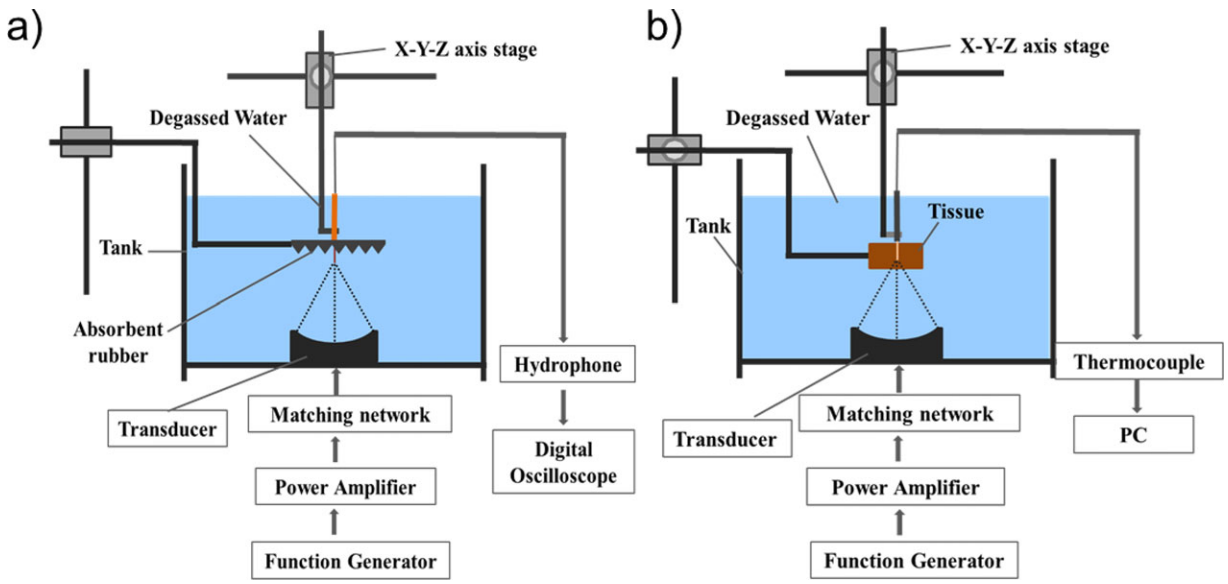


**FIG. 2** *Schematic diagram of the experimental setup for measuring focused ultrasound induced pressure and tissue temperature. (a) Pressure measurement using a needle-type hydrophone. (b) Temperature measurement using a thermocouple.*

**TABLE 1** ***Material parameters used in the simulation [18–20]***

| *Material* | *Symbol* | *Value* | *Unit* |
|---|---|---|---|
| PZT type | PZT-4 | – | – |
| Specific heat of blood | $C_b$ | 3,770 | J(kg·C) |
| Specific heat of muscle | $C_m$ | 3,770 | J(kg·C) |
| Thermal conductivity of muscle | $k$ | 0.5 | W/(m·C) |
| Blood perfusion rate | $w_b$ | 0.5 | kg/(m$^3$·Sec) |
| Attenuation coefficient of water | $a_w$ | 0.025 | Np/(m·MHz) |
| Attenuation coefficient of muscle | $a_m$ | 4.1 | Np/(m·MHz) |
| Speed of sound in acoustic lens | $c_{lens}$ | 7,500 | m/Sec |
| Speed of sound in water | $c_w$ | 1,480 | m/Sec |
| Speed of sound in muscle | $c_m$ | 1,575 | m/Sec |
| Density of water | $\rho_w$ | 998 | kg/m$^3$ |
| Density of muscle | $\rho_m$ | 1,070 | kg/m$^3$ |
| Young's modulus of muscle | $E$ | 5,000 | Pa |

verified using 3-(4,5-dimethylthiazol-2-yl)-2,5-diphenyltetrazolium bromide (MTT) assay. First, 4T1 (breast cancer) and CT26 (colon cancer) cells were grown in 48-well plates at a density of $3 \times 10^4$cells/well in 300 μL of a culture medium. The cultured cells were divided into five groups: the negative control group, drug-unloaded microbead group, ultrasound-only group, drug-loaded microbead group, and drug-loaded microbeads with ultrasound induction group. Before treatment, all groups were maintained overnight in an incubator for attachment of the cultured cells. After 24 H, the used medium was replaced with alginate microbeads distributed culture medium or new medium. Next, the focused

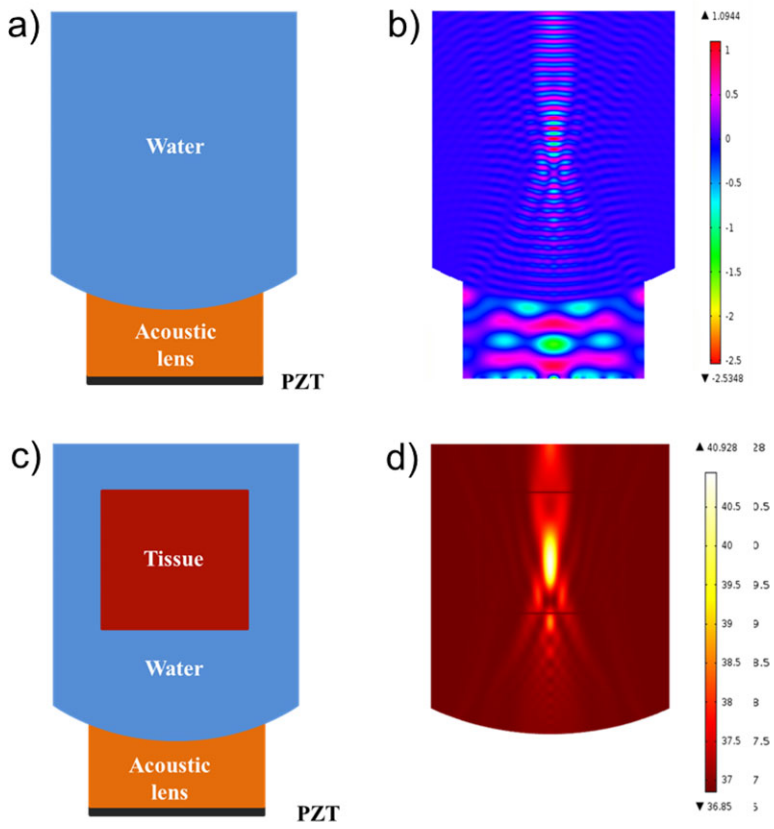


**FIG. 3** *COMSOL simulation model and simulation results images: (a and c) 2D models of focused ultrasound induced pressure and tissue temperature. (b and d) Simulation result images of focused ultrasound induced pressure and tissue temperature.*

ultrasound system setup was prepared as in previous experiments, and the 48-well plate was fixed with the XYZ stage holder and placed 29.5 mm above the transducer [22]. Then, ultrasound was applied for 4 Min at the selected parameter to the ultrasound-only and drug-loaded microbeads with ultrasound induction groups. After the cells were further cultured for 24 H in the incubator, cell viability was measured using MTT assay.

### 2.6. Focused ultrasound enhanced drug uptake

Enhanced intracellular uptake of DTX by the focused ultrasound was quantitatively analyzed by the HPLC method [23]. 4T1 and CT26 cells were seeded in 48-well plates and incubated for overnight. The used medium was replaced by the 300 μL culturing medium with drug concentration of 20 μg/mL alginate microbeads. Then, the focused ultrasound was applied to the corresponding samples for 4 Min. and the samples without ultrasound treatment were set as controls. After further incubation for 2 H at 37 °C, the cells were washed three times with ice-cold PBS solution. Subsequently, the total proteins of cells were extracted by adding SDS (0.2%) solution and incubated for 30 Min at 37 °C. The protein amount of the cell lysates was measured using bicinchoninic acid assay. Next, each sample was mixed with equal volume of acetonitrile and vortexed for 10 Min and the sample was prepared for HPLC analysis.

## 3. Results and Discussion

Figures 3a and 3b show scanning electron microscopy (SEM) images of the PLGA-DTX nanoparticles and the PLGA-DTX-encapsulated alginate microbeads, respectively. In Fig. 3a, the PLGA-DTX nanoparticles have a uniform spherical morphology, and the mean size of the nanoparticles is approximately 344 nm (Fig. 3c). In addition, the PLGA-DTX alginate microbeads also have a smooth spherical morphology with mean diameter of 4.5 μm in Figs. 3b and 3d, The drug encapsulation efficiency of alginate microbeads was 1.75 ± 0.35 wt%.

The images from the COMSOL simulation results are shown in Figs. 2b and 2d, and the COMSOL simulation results (generated pressure and temperature) are compared with the experimental data in Figs. 4 and 5. The COMSOL simulation showed similar results as the experimental data, as shown in Figs. 4 and 5. The discrepancies between the simulation and the experiment could have been caused by the differences in the material properties and the modeling errors in the focused ultrasound device. In addition, after the degassing of the water in the experiment, some gas remained in the water, which could have affected the experimental data.

To search the appropriate parameters of focused ultrasound for drug delivery, the experimental and simulation data were analyzed and evaluated using contact method. First,

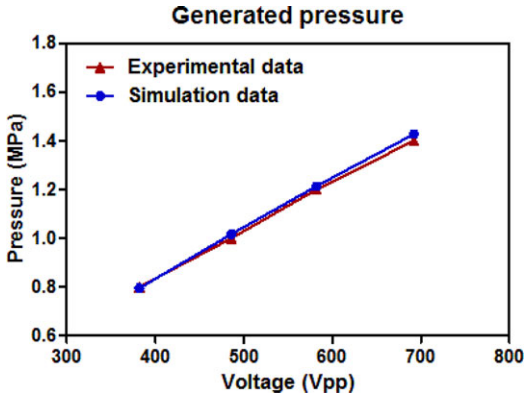


**FIG. 4** *Experimental and simulation results of focused ultrasound induced pressure by input voltage. The experimental data were measured with a needle-type hydrophone.*

as the input voltage of the focused ultrasound increased, the peak pressure also increased (Fig. 4). Second, the generated positive and negative pressures were similar when the focused ultrasound operated with all the sonication conditions used in this study. This result is in accordance with results reported by other researchers [24, 25]. Third, as shown in Figs. 5a and 5b, when the output peak pressures were 0.8 and 1 MPa, the tissue temperature increased to 39.4 and 40.7 °C, respectively. After approximately 200 Sec, the tissue temperature ceased to rise because it had reached thermal equilibrium. However, when the peak pressure was 1.2 and 1.4 MPa, the generated tissue temperatures easily rose above 42 °C (Figs. 5c and 5d). Therefore, the peak pressure of 1.2 and 1.4 MPa was not reasonable for focused ultrasound induced drug delivery because significant vascular shutdown can occur at 43 °C [26].

In addition, Fig. 6a shows the drug release rates induced by ultrasound according to the peak pressure. When the output pressure increased, the drug release rate also increased. Because, when the negative acoustic pressure increased, the cavitation effect can be enhanced. In addition, when the burst period increased, the drug release rate was significantly reduced, and the highest release rate can be achieved when the period was 12 μ Sec (Fig. 6b). However, at the burst period of

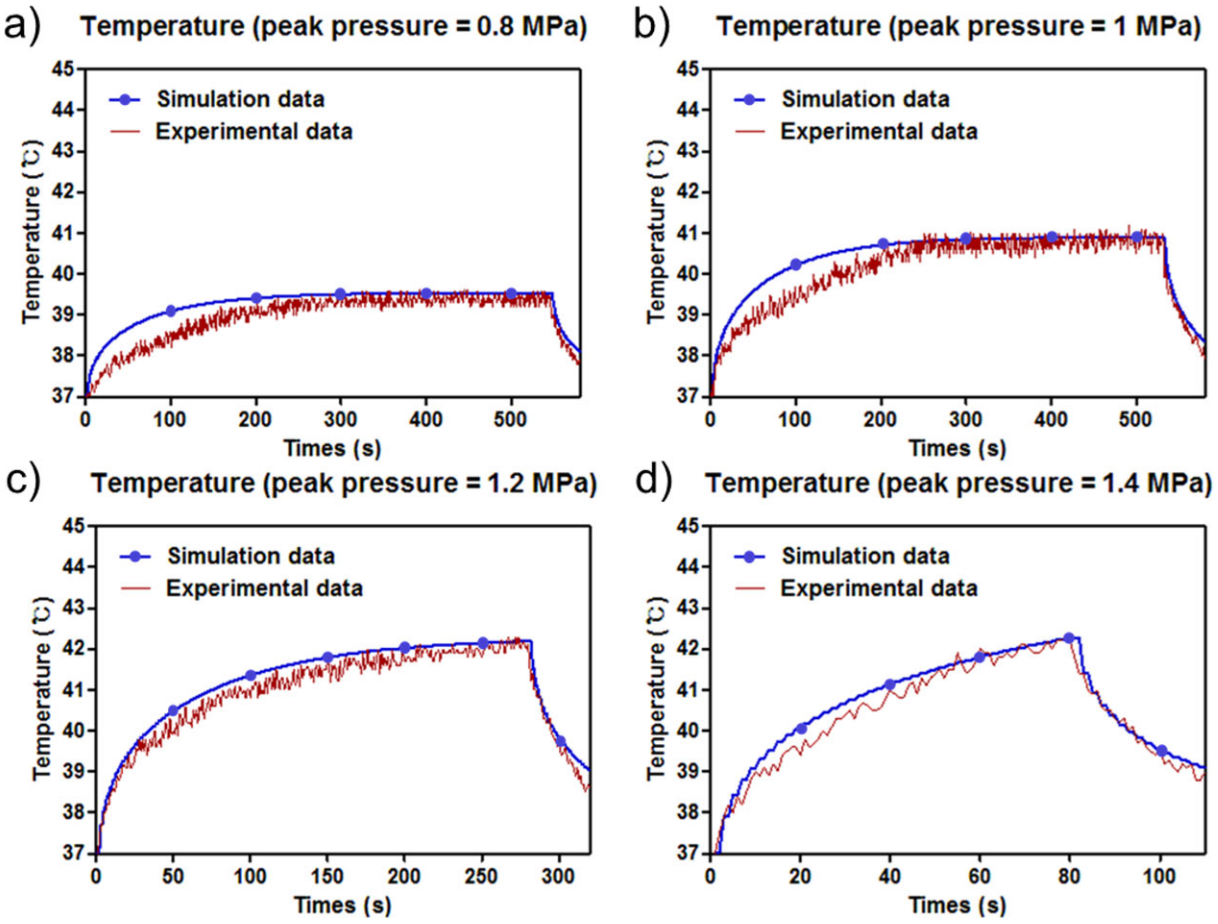


**FIG. 5** *Simulation and experimental results of focused ultrasound induced tissue temperature: (a–d) Tissue temperature changes at peak pressure of 0.8, 1, 1.2, and 1.4 MPa. The temperature was measured with a thermocouple (UT-325), and the input power was stopped manually when the temperature reached 42 °C or thermal equilibrium occurred.*

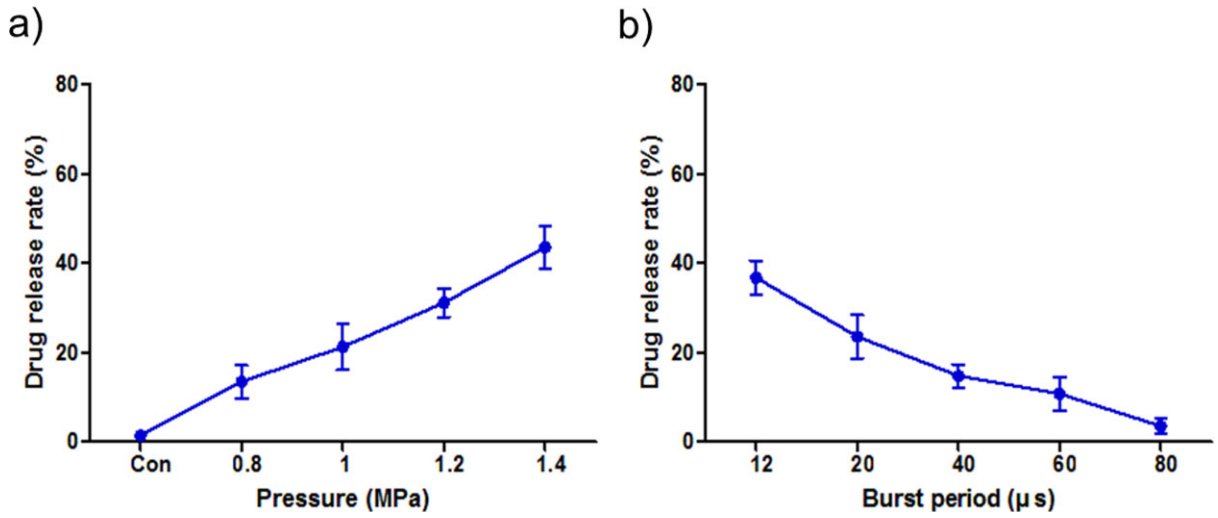


**FIG. 6** *Focused ultrasound induced drug release. (a) Drug release rate upon to peak pressure with fixed burst period of 20 μs and 10 cycles. (b) Drug release rate according to burst period when the pressure is 1 MPa and the number of cycle is 10. Ultrasound treatment time for all samples was 4 Min.*

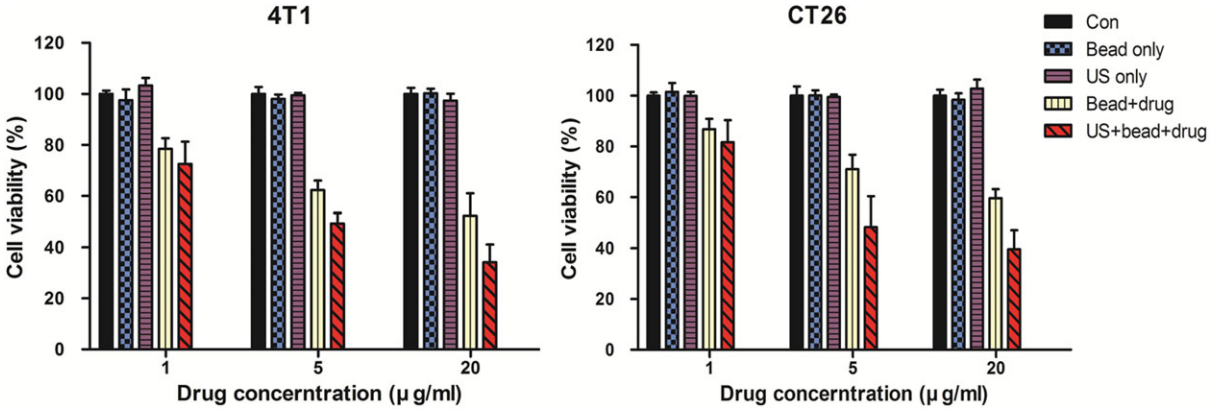


**FIG. 7** *Viability of 4T1 and CT26 cells after treatment with drug-unloaded microbeads, ultrasound, drug-loaded microbeads, and focused ultrasound combined with drug-loaded microbeads.*

12 μ Sec, the tissue temperature was increased more than 42 °C in 2 Min. Finally, based on the simulation and experimental results for the generated pressure, tissue temperature, and drug release, we selected the following ultrasound parameters, such as the output peak pressure of 1 MPa, 10 cycles per burst, and the burst period of 20 μ Sec. Then, the resulting generated output power became about 4.2 W for the focused ultrasound drug delivery.

We performed cytotoxicity tests and drug uptake test to confirm the ultrasound-enhanced drug delivery. Figure 7 shows the results of the cell viability with the focused ultrasound and the DTX alginate microbeads using MTT assay. The drug-unloaded microbead (bead-only) group and the group showed no significant differences with the control groups. However, the drug-loaded alginate microbead and the drug-loaded microbead with ultrasound induction groups exhibited a clear antitumor effect. Additionally, the drug-loaded microbead with ultrasound induction group displayed a significant higher antitumor effect than the drug-loaded microbead group without ultrasound induction. In addition, the drug uptake efficiency of 4T1 and CT26 cells with ultrasound induction also showed 3.4- and 2.6-fold higher than without ultrasound induction, as shown in Fig. 8. Actually, the temperature of culture medium in the cell culture dish increased less than 2 °C due to the low acoustic absorption coefficient of cell culture media [18], when the ultrasound was operated with the peak pressure of 1 MPa and the burst period of 20 μSec. Therefore, the enhancement of cell killing effect and drug uptake cannot be caused by heat effect. The generated pressure was also decreased about 18.2% due to the ultrasound reflection by cell culture plate. However, when the peak pressure is 1 MPa, the decreased pressure was about 0.82 MPa, which is much higher than 0.5 MPa (the lowest pressure for the generation of cavitation effect) [27, 28]. Therefore, the pressure from focused ultrasound can still generate the cavitation effect to increase the drug release

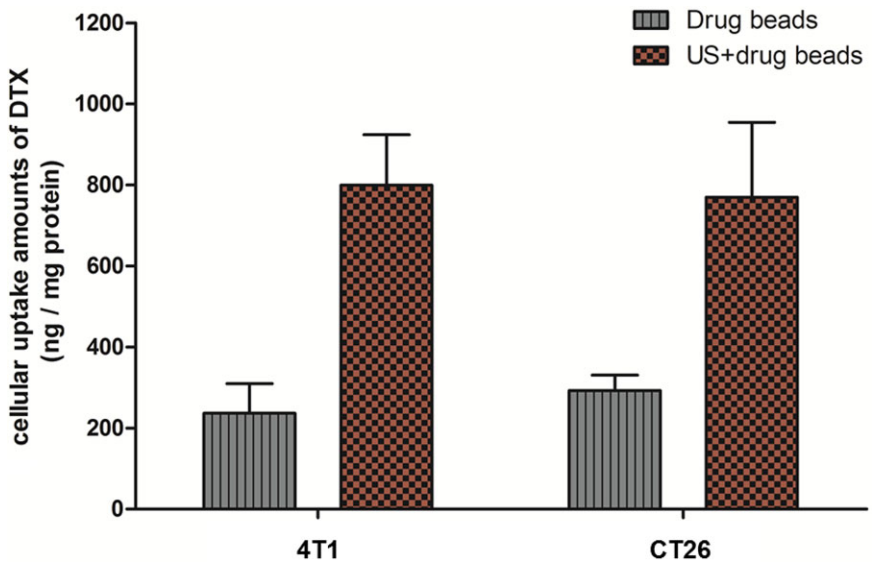


**FIG. 8**

*In vitro cellular uptake studies of DTX in 4T1 and CT26 cell. Drug beads with cell line after ultrasound treatment or without ultrasound treatment were incubated for 2 H. The cellular uptake amounts of DTX were analyzed by the HPLC system, and then they were normalized by protein amounts measured by bicinchoninic acid (BCA) assay.*

and drug uptake. In addition, the drug release and drug uptake can be enhanced by an acoustic streaming effect [29, 30] and the cell membrane's permeability can be also enhanced by the sonoporation effect [10, 31, 32].

## 4. Conclusions

In this research, we conducted experimental and simulation studies on focused ultrasound triggered drug delivery. First, we fabricated PLGA-DTX-encapsulated alginate microbeads as a drug carrier and installed a focused ultrasound setup with pressure and temperature sensors. Second, we developed simulation models for focused ultrasound induced pressure and tissue temperature using COMSOL Multiphysics 4.3a. Third, we evaluated the drug release rate using focused ultrasound and determined the appropriate parameters for focused ultrasound drug delivery based on an analysis of the results from the generated pressure and tissue temperature and the drug release rate. Finally, through *in vitro* tests using tumor cells (4T1 and CT26), we confirmed the antitumor effect of PLGA-DTX-encapsulated alginate microbeads combined with focused ultrasound induction. The PLGA-DTX-encapsulated alginate microbeads with ultrasound induction had significant higher antitumor effect than the PLGA-DTX-encapsulated alginate microbeads without ultrasound treatment. Consequently, it is expected that focused ultrasound can be an effective induction method for antitumor drug delivery.

## 5. Acknowledgements

This work was supported by the Samsung Research Funding Center for Future Technology under Project Number SRFC-IT1401-06.

## 6. References

[1] Chen, T., Shukoor, M. I., Wang, R., ZHAO, Z., and Yuan, Q. (2011) ACS Nano 5, 7866–7873.
[2] Poste, G., and Kirsh, R. (1983) Nat. Biotechnol. 1, 869–878.
[3] Kooa, H., Mina, K. H., Lee, S. C., Park, J. H., and Jeong, S. Y. (2013) J. Control. Release 172, 823–831.
[4] Tietze, R., Lyer, S., S Dürr, S., Struffert, T., and Engelhorm, T. (2013) Nanomed. Nanotechnol. 9, 961–971.
[5] Geers, B., Lentacker, I., Sanders, N. N., Demeester, J., and Mearis, S. (2011) J. Control. Release 152, 249–256.
[6] Mackowiak, S. A., Schmidt, A., Weiss, V., Christian, A., Schirndaing, C. V., Bein, T., and Brauchle, C. (2013) Nano Lett. 13, 2576–2583.
[7] Gong, R., Li, C., Zhu, S., Zhang, Y., Yan, D., and Jiang, J. H. (2011) Carbohydr. Polym. 85, 869–874.
[8] Oliveira, H., Pérez-Andrés, E., Thevenot, J., Sandre, O., and Berra, E. (2013) J. Control. Release 169, 165–170.
[9] Liu, T.Y., and Huang, T. C. (2011) Acta Biomater. 7, 3927–3934.
[10] Grüll, H., and Langereis, S. (2012) J. Control. Release 161, 317–327.
[11] Li, G., Fei, G., Xia, H., Han, J., and Zhao, Y. (2012).J. Mater. Chem. 22, 7692–7696.
[12] Lentacker, I., Cock, I. D., Deckers, R., Smedt, S. C. D., and Moonen, C. T. W. (2014) Adv. Drug Deliver. Rev. 72, 49–64.
[13] Zhang, H., Xia, H., Wang, J., and Li, Y. W. (2009) J. Control. Release 139, 31–39.
[14] Cool, S. K., Geers, B., Roels, S., Stremersch, S., Vanderperren, K., and Saunders, J. H. (2013) J. Control. Release 172, 885–893.
[15] Stieger, S. M., Caskey, C. F., Adamson, R. H., Qin, S., Curry, F. R., Wisner, E. R., and Ferrara, K. W. (2007) Radiology 243, 112–121.
[16] Keum, C. G., Noh, Y. W., Baek, J. S., Lim, J. H., Hwang, C. J., and Na, Y. G. (2011) Int. J. Nanomed. 6, 2225–2234.
[17] Fusco, S., Sakar, M.S., Kennedy, S., Peters, C., Bottani, R., and Starsich, F. (2014) Adv. Mater. 26, 952–957.
[18] Heikkila, J., Curiel, L., and Hynynen, K. (2010) IEEE Trans. Biomed. Eng. 57, 785–793.

[19] Damianou, C. A., Sanghvi, N. T., Fry, F. J., and Maass-Moreno, R. (1997) J. Acoust. Soc. Am. 102, 628–634.
[20] Hallaj, I. M., Cleveland, R. O., and Hynynen, K. (2001) J. Acoust. Soc. Am. 109, 2245–2249.
[21] Jin, D., Jennifer, P., Xiao, G., Jiang, X. N., and Jing, Y. (2014) Adv. Healthcare Mater. 3, 811–816.
[22] Lo, C. W., Desjouy, C., Chen, S. R., Lee, J. L., Inserra, C., and Béra, J. C. (2014) Ultrason. Sonochem. 21, 833–839.
[23] Cho, H. J., Yoon, H. Y., Koo, H., Ko, S. H., Shim, J. S., Lee, J. H., and Kim, D. D. (2011) Biomaterials 32, 7181–7190.
[24] Bailey, M. R., Couret, L. N., Sapozhnkov, O. A., Khokhlova, V. A., Ter Haar, G., and Vaezy, S. (2001) Ultrasound Med. Biol. 27, 695–708.
[25] Chen, W. S., Brayman, A. A., Matula, T. J., Crum, L. A., and Miller, M. W. (2002) Ultrasound Med. Biol. 29, 739–748.
[26] Vaupel, P. W., and Kelleher, D. K. (2010) Int. J. Hyperther. 26, 211–223.
[27] Coussios, C. C., Farny, C. H., Ter Haar, G., and Roy, R. A. (2007) Int. J. Hyperther. 23, 105–120.
[28] Gruber, M. J., Bader, K. B., and Holland, C. (2014) J. Acoust. Soc. Am. 135, 646–648.
[29] Azagury, A., Khoury, L., Enden, G., and Kost, J. (2014) Adv. Drug Deliv. Rev. 72, 127–143.
[30] Husseini, G. A., Runyan, C. M., and Pitt, W. G. (2002) BMC Cancer 2, 20–25.
[31] Liang, H. D., Tang, J., and Halliwell, M. (2010) Med. Phys. 224, 343–361.
[32] Douglas, L., Miller, D. L., Pislaru, S. V., and Greenleaf, J. F. (2002) Somat. Cell Mol. Genet. 27, 115–134.